University of Groningen

γ-ray diagnostics of α slowing in inertial confinement fusion targets

Dendooven, Peter; Drake, R. Paul; Cable, Michael D.

γ-ray diagnostics of α slowing in inertial confinement fusion targets

Peter G. Dendooven, R. Paul Drake, and Michael D. Cable

γ-ray diagnostics of α slowing in inertial confinement fusion targets

Peter G. Dendooven
Plasma Physics Research Institute, University of California, Lawrence Livermore National Laboratory, P.O. Box 5508, Livermore, California 94550

R. Paul Drake
Plasma Physics Research Institute, Lawrence Livermore National Laboratory and University of California, Davis, P.O. Box 5508, Livermore, California 94550

Michael D. Cable
University of California, Lawrence Livermore National Laboratory, P.O. Box 5508, Livermore, California 94550

For large inertial confinement fusion deuterium-tritium targets, a way to diagnose α slowing might be via capture reaction γ rays. Calculations are presented for two such methods: one uses the α+T direct capture γ rays, the other is based on a series of resonant α-capture reactions. For small targets ($\rho R < 0.02$ g/cm^2), the total α+T γ-ray yield relative to the DT neutron yield is temperature independent and proportional to the ρR value. For large targets ($\rho R \geqslant 0.2$ g/cm^2), this quantity becomes temperature dependent and ρR independent. Some experimental aspects are discussed.

I. INTRODUCTION

Fuel heating by energetic reaction products is a requirement for efficient thermonuclear burn in both magnetic and inertial confinement fusion (ICF) devices. Therefore, for deuterium-tritium (DT) fusion, the stopping of the 3.5 MeV α particles in the fuel is very important and diagnostic techniques for the α slowing should be developed. Various techniques have been suggested (and some of them implemented) in connection with magnetic confinement fusion. The methods based on charge exchange reactions between α particles and neutral-atom beams[1,2] are useless in ICF research. Techniques based on nuclear reactions, on the other hand, are useful for both fusion approaches, although the experimental requirements are quite different. Slaughter[3] gives an extensive list of nuclear reactions between α particles in the 0.5–3.5 MeV energy range and light ions resulting in the emission of penetrating γ rays or neutrons. Cecil *et al.*[4,5] describe the use of γ rays from a series of resonant α-capture reactions with different resonance energies. Kiptilyj[6] proposes a method based on the Doppler shape analysis of the 4.44 MeV γ ray from the ^{9}Be($\alpha,n_1\gamma$)^{12}C reaction. Up to now, nuclear techniques have primarily been used to investigate the behavior of fast particles other than α particles in magnetically confined plasmas.[7-10]

We present here the results of the first investigation into diagnostic methods for α slowing in ICF targets based on α-capture γ rays. Section II summarizes the relevant properties of capture reactions. Section III describes the use of the $\alpha+T \rightarrow {}^7Li+\gamma$ direct capture reaction. The ICF target yields for a series of resonant reactions are presented in Sec. IV. Section V discusses some experimental aspects.

II. CAPTURE REACTIONS

A. General expression for the capture γ-ray energy spectrum

Consider a capture reaction $1+2 \rightarrow 3+\gamma$. Conservation of energy in the center-of-mass system gives

$$E'_\gamma + E'_3 = E'_1 + E'_2 + Q, \tag{1}$$

where the prime denotes the kinetic energy in the center-of-mass system and Q is the reaction Q value (total initial minus final mass). Using conservation of momentum, we obtain

$$E'_\gamma = E^0_3 \left[-1 + \left(1 + \frac{2(E'+Q)}{E^0_3} \right)^{1/2} \right], \tag{2}$$

where $E' = E'_1 + E'_2$ and E^0_3 is the rest energy of the final nuclear state (most often the ground state). Transformation to the laboratory system gives the observed γ-ray energy as

$$E_\gamma = E'_\gamma \left[\frac{(1-\beta^2)^{1/2}}{1-\beta \cos\theta} \right], \tag{3}$$

where $\beta \equiv V/c$ with V the velocity of the center of mass and c the speed of light; θ is the angle between V and the detector.

From Eqs. (2) and (3) it follows that different combinations of E', V, and $\cos\theta$ can give the same γ-ray energy. Thus, the γ-ray energy spectrum is given by

$$P_\gamma(E_\gamma)dE_\gamma = \int_{V_{min}}^{V_{max}} \xi(V)dV \int_{E'_{min}}^{E'_{max}} \phi(E')P_r(E')dE'$$

$$\times \psi(\mu) \frac{d\mu}{dE_\gamma} dE_\gamma, \tag{4}$$

where $P_\gamma(E_\gamma)dE_\gamma$ is the probability the γ-ray energy lies between E_γ and $E_\gamma+dE_\gamma$, $\xi(V)dV$ is the (normalized) distribution of the velocity of the center of mass, $\phi(E')$ is the (normalized) probability to have a reaction energy E', $P_r(E')dE'$ is the reaction probability between energies E' and $E'+dE'$ (it is assumed this depends only on E'), and $\psi(\mu)d\mu$ is the (normalized) γ-ray angular distribution ($\mu\equiv\cos\theta$). At a certain V, the energy integration runs over all reaction energies for which there is a μ that gives a γ-ray energy equal to E_γ.

Equations (1), (2), and (4) are only valid if the final nuclear state has a zero natural linewidth (i.e., a long half-life). If not, an additional γ-ray energy distribution according to this linewidth must be taken into account.

B. Direct and resonant capture reactions

A direct capture reaction is a one-step process in which there is a direct transition from initial to final state accompanied by the emission of a γ ray. A resonant capture reaction is a two-step process: first, a compound nucleus is created in an excited state, then this state decays via particle emission or electromagnetic transitions (where the γ rays originate).

Direct capture can occur at all projectile energies. At low energies, the cross section for charged-particle-induced direct capture reactions is dominated by the Coulomb barrier penetration factor. It is therefore convenient to factor out this energy dependence and express the cross section $\sigma(E')$ as

$$\sigma(E')=\frac{S(E')}{E'}\exp[-(E_G/E')^{1/2}],\qquad(5)$$

with the Gamow energy E_G given by

$$E_G=0.9791Z_1^2Z_2^2\frac{A_1A_2}{A_1+A_2}\ \text{MeV},\qquad(6)$$

where Z_1, Z_2 are the atomic numbers and A_1, A_2 the mass numbers of the reacting nuclei. Cross sections are then conveniently discussed in terms of the astrophysical factor $S(E')$.

When the energy in the entrance channel ($E'+Q$) matches the energy of a state in the compound nucleus, resonant capture may occur (angular momentum and parity conservation laws also play a role). The cross section for the resonant reaction $1+2\rightarrow3+4$ as a function of the reaction energy is given by the Breit–Wigner formula (all energies and widths are in the center-of-mass system)

$$\sigma(E')=\pi\lambda^2\frac{2J+1}{(2J_1+1)(2J_2+1)}\frac{\Gamma_{12}\Gamma_{34}}{(E'-E'_R)^2+(\Gamma/2)^2},\qquad(7)$$

where $\lambda=\hbar/(2mE')^{1/2}$ is the reduced de Broglie wavelength, m is the reduced mass of the reactants, J_1 and J_2 are the angular momenta of the initial nuclear states, J is the angular momentum of the resonant state in the compound nucleus, and E'_R is the resonance energy. $\Gamma=\Gamma_{12}+\Gamma_{34}+\cdots$ (all other possible decay channels) is the total width of the resonant state. Γ_{12} is the partial
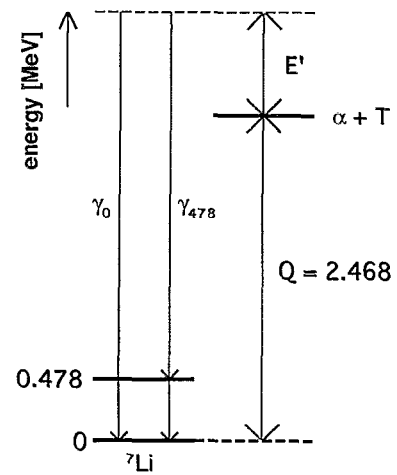

FIG. 1. Center-of-mass energy relationship for the $\alpha+T$ capture reaction. All energies are in MeV.

width for the reemission of 1 and 2 (elastic scattering) and Γ_{34} is the partial width for the emission of 3 and 4. This width can refer to particle as well as γ-ray emission. The total capture cross section consists of resonances superposed on a smooth direct capture "background." A more extensive overview of charged-particle reactions at energies relevant to fusion research can be found in Ref. 11.

III. $\alpha+T$ CAPTURE γ RAYS

A. The $\alpha+T\rightarrow{}^7Li+\gamma$ reaction

Below 3.5 MeV α energy, the $\alpha+T$ reaction is purely direct capture with a constant astrophysical factor[12] equal to 0.064 keV b. The reaction has two channels: directly to the ground state, resulting in the emission of a γ_0 and to the first excited level of ^7Li at 478 keV, resulting in a γ_{478} and a consequent 478 keV γ ray (Fig. 1). Griffiths et al.[12] measure a drop of the γ_{478}/γ_0 branching ratio from 0.45 to 0.36 when the α energy decreases from 1.32 to 0.56 MeV. Since these two values are inadequate to determine a good energy dependence of the branching ratio, the calculations described in Sec. III C assume it to be constant and equal to 0.45.

B. Relationship between α slowing and γ-ray energy spectrum

When considering the α slowing in a thermalized plasma, the motion of the plasma nuclei is assumed to be negligible compared to that of the α particles. In this case ($E_T=0$), we have

$$E'=\frac{m_T}{m_\alpha+m_T}E_\alpha\qquad(8)$$

and

$$V=\frac{(2m_\alpha E_\alpha)^{1/2}}{m_\alpha+m_T}.\qquad(9)$$

Because of this one-to-one relationship between V and E_α, one integration disappears from Eq. (4) and the γ-ray energy spectrum is given by

$$P_\gamma(E_\gamma)dE_\gamma = \int_{E_\alpha^{\min}}^{E_\alpha^{\max}} \phi(E_\alpha)P_r(E_\alpha)dE_\alpha \, \psi(\mu)\frac{d\mu}{dE_\gamma} dE_\gamma.$$

$$(10)$$

The reaction probability is given by

$$P_r(E_\alpha)dE_\alpha = \frac{N_A}{A_f} \frac{\sigma(E_\alpha)}{|dE_\alpha/d(\rho x)|} dE_\alpha,$$

$$(11)$$

where A_f is the fuel mass number, N_A is the Avogadro's constant ($=6.022\times10^{23}$/mol), $\sigma(E_\alpha)$ is the reaction cross section, and $|dE_\alpha/d(\rho x)|$ is the specific stopping power [MeV/(g/cm^2)].

The symbol ρx designates the areal density along some α trajectory. In general, this is the integral of the density along the trajectory. If the fuel consists of a mixture (or compound) of one active (subscript 1) and a number of inactive elements, Eq. (11) becomes

$$P_r(E_\alpha)dE_\alpha = \frac{f_1 N_A}{\Sigma_i f_i A_i} \frac{\sigma(E_\alpha)}{|dE_\alpha/d(\rho x)|} dE_\alpha,$$

$$(12)$$

where A_i is the mass number and f_i the relative density (number of nuclei/cm^3) of the ith element ($\Sigma f_i = 1$). The stopping power is that for the mixture or compound, which is equal to the sum of the stopping powers for the individual elements, each weighed by the weight fraction $f_i A_i/\Sigma_i f_i A_i$. Equations (10)–(12) show that the $\alpha + T$ capture γ-ray energy spectrum depends on the reaction cross section, the α stopping power in the fuel and the energy distribution of the α particles. Thus, if the two former are known, the latter can be determined from the γ-ray spectrum. This is analogous to the use of secondary DT neutrons from DD fuel for measuring the triton slowing.[13]

C. Calculations for different burn distributions

The α energy distribution $\phi(E_\alpha)$ depends on the burn distribution and the fuel density distribution. Following Cable and Hatchett,[13] $\phi(E_\alpha)$ is written in terms of the probability that an α particle traverses a fuel areal density between ρx and $\rho x + d(\rho x)$ before leaving the fuel, $P_{\rho x}(\rho x)d(\rho x)$:

$$\phi(E_\alpha) = \int_{\rho x(E_\alpha)}^{\rho x(0)} P_{\rho x}(\rho x)d(\rho x)$$

$$= 1 - \int_0^{\rho x(E_\alpha)} P_{\rho x}(\rho x)d(\rho x),$$

$$(13)$$

where

$$\rho x(E_\alpha) = \int_{E_\alpha^0}^{E_\alpha} \frac{dE_\alpha}{dE_\alpha/d(\rho x)}$$

$$(14)$$

is the amount of fuel needed to slow the α's from their initial energy E_α^0 ($=3.5$ MeV) down to an energy E_α. Inverting this relationship gives

$$E_\alpha(\rho x) = E_\alpha^0 - \int_0^{\rho x} \frac{dE_\alpha}{d(\rho x)} d(\rho x).$$

$$(15)$$

Equation (13) is only valid if the fraction of α particles that reacts is small. Because of the small $\alpha + T$ cross section, this is always the case.

Using the above formulas, we calculated the $\alpha + T$ γ-ray spectrum for different burn distributions. These calculations, using Monte Carlo techniques, proceed as follows:

(1) choose ρx according to $P_{\rho x}(\rho x)$,

(2) calculate the final α energy after crossing an amount of fuel equal to ρx,

(3) choose an α reaction energy randomly between the final α energy and 3.5 MeV,

(4) calculate the reaction probability at this energy using Eq. (12),

(5) choose one of the two γ-ray branches according to 69% γ_0 and 31% γ_{478},

(6) choose $\cos\theta$ according to an isotropic angular distribution,

(7) calculate the γ-ray energy using Eqs. (2) and (3),

(8) digitize the γ-ray energy (determine the spectrum channel),

(9) add the reaction probability to the spectrum channel.

Repeating these steps a large number of times (typically 10^5) creates a γ-ray energy spectrum. The α stopping power, which is strongly temperature and weakly density dependent, was calculated according to Sivukhin.[14] In the following, the results of the calculations for two burn distributions are given and discussed.

1. The hot spot model

In the hot spot model it is assumed that the reaction products are produced at a point at the center of a sphere of radius ρR (g/cm^2) with time- and space-independent temperature and density. This is consistent with an implosion where the burn occurs in a small, high-temperature "hot spot" surrounded by colder fuel mass. In this case, all reaction products traverse the same amount of fuel, thus

$$P_{\rho x}(\rho x)d(\rho x) = \delta(\rho x - \rho R)d(\rho x)$$

$$(16)$$

$$\phi(E_\alpha) = 1 \quad \rho x(E_\alpha) < \rho R$$

$$= 0 \quad \rho x(E_\alpha) > \rho R.$$

$$(17)$$

Figure 2(a) shows the calculated γ-ray spectra for different ρR values for a fuel density of 21 g/cm^3 and a temperature of 5 keV. The 478 keV γ ray is not shown since its shape hardly changes as a function of ρR. The ratio of the γ-ray yield and the primary neutron yield as a function of ρR for different temperatures is given in Fig. 3. The plotted γ-ray yield does not include the 478 keV γ ray. Due to the weak density dependence of the α stopping power, the density dependence of the γ-ray yield is quite small.
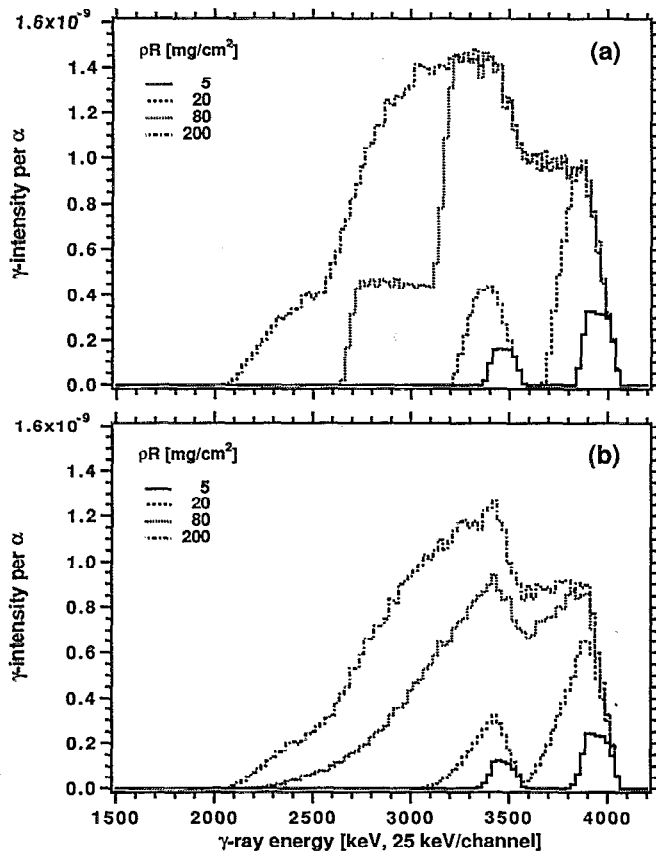
FIG. 2. Simulated $\alpha+T$ capture γ-ray energy spectra in the hot spot (a) and uniform burn (b) models for different ρR values. The calculations were performed for a density of 21 g/cm³ and a temperature of 5 keV.

2. Uniform burn of spherical fuel

In the case of the uniform burn of spherical fuel with uniform temperature and density and an areal density ρR, it can be shown that
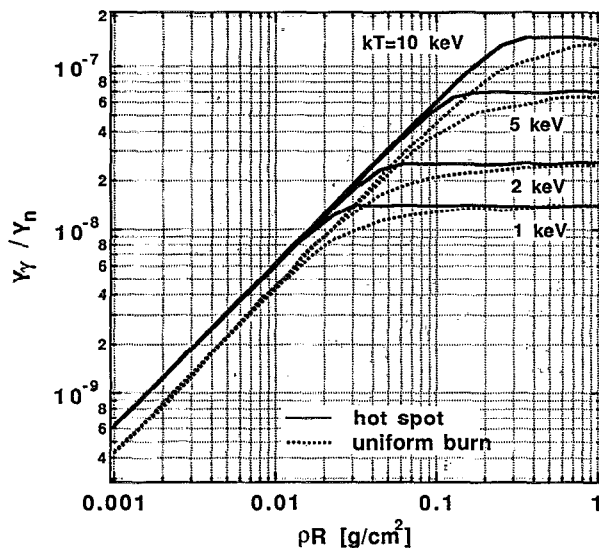

FIG. 3. Ratio of the $\alpha+T$ γ ray and D+T neutron yield vs ρR for different temperatures in the hot spot and uniform burn models for a density of 21 g/cm³.

$$P_{\rho x}(\rho x)d(\rho x)=\frac{3}{4\rho R}\left[1-\frac{1}{4}\left(\frac{\rho x}{\rho R}\right)^2\right]d(\rho x), \quad (18)$$

$$\phi(E_\alpha)=1-\frac{3\rho x(E_\alpha)}{4\rho R}+\frac{1}{16}\left(\frac{\rho x(E_\alpha)}{\rho R}\right)^3. \quad (19)$$

Figure 2(b) shows the γ-ray spectra calculated using this model. The ratio of the γ-ray yield and the primary neutron yield as a function of ρR for different temperatures is given in Fig. 3.

3. Discussion

The fuel ρR value can be determined from the γ-ray energy where the intensity drops to half of its maximum value (at the low-energy side of the maximum). This half-maximum point is rather insensitive to the burn distribution. This method of ρR measurement breaks down for target sizes such that most α particles are completely stopped.

At small ρR values (the linear part in Fig. 3), Y_γ/Y_n is temperature independent, although the α energy loss is highly temperature dependent. The reason for this is the fact that the $\alpha+T$ capture reaction cross section drops little over the α energy interval covered at these small ρR values. The α energy has to drop from 3.5 to 0.9 MeV for the cross section to drop by a factor of 2. The measurement of Y_γ/Y_n thus results in a temperature-independent determination of ρR. There is, however, a small dependence on the burn distribution. A fit for ρR below 0.032 g/cm² gives the following results:

hot spot: $Y_\gamma/Y_n=6.1\times10^{-7}\rho R$,

uniform burn: $Y_\gamma/Y_n=4.7\times10^{-7}\rho R$.

The fitted exponent of ρR is, as expected, equal to 1 (within the error). The total yield in the uniform burn model is 77% of that in the hot spot model, reflecting the fact that the average ρx for a uniform burn is equal to $3/4\rho R$. Since any burn distribution with its maximum at the center of the fuel results in γ-ray yields between the hot spot and uniform burn models, the error due to the uncertainty in the burn distribution is rather small (at most 15% around $\rho R=0.01$ g/cm²).

For ρR values larger than the range of the α particles, Y_γ/Y_n depends less and less on ρR (for a hot spot model, Y_γ/Y_n actually becomes constant), but is strongly temperature dependent. This is the result of the decreasing stopping power (increasing range) with increasing temperature. In this region, Y_γ/Y_n can be used to estimate the temperature without accurate knowledge of ρR and the burn distribution.

In extracting ρR values from the γ-ray spectra, one needs to know the stopping power of the α particles in the fuel. Consequently, if one knows the ρR value from some other measurement, γ-ray spectra can give information on the stopping power.
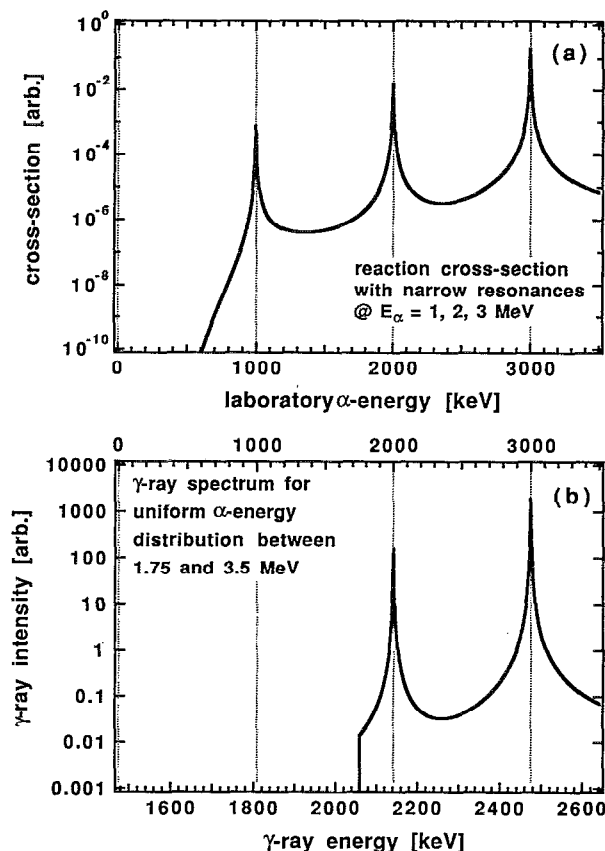
FIG. 4. Illustration of the relationship between the α-energy distribution and the center-of-mass capture γ-ray energy spectrum when the cross section shows a series of narrow resonances. (a) The cross section vs α energy. (b) The γ-ray intensity vs γ-ray energy (bottom axis) and α energy (top axis) (in the center of mass, there is a one to one relationship between γ and α energy).

IV. THE USE OF A SERIES OF NARROW RESONANCES

The center-of-mass α-capture γ-ray energy spectrum is proportional to the product of the reaction cross section and the α particle energy distribution. A narrow resonance in the cross section thus results in a narrow γ-ray peak in the spectrum, who's intensity is proportional to the number of α particles with an energy equal to the resonance energy. In the laboratory frame, the Doppler effect broadens this peak. If an ICF target contains nuclei with which the α particles undergo a series of resonances, the intensities of the different γ-ray peaks give the number of α particles slowed down to the different resonance energies, i.e., a "stepwise" picture of the α slowing is obtained. This is illustrated in Fig. 4.

The only resonant α-capture reaction below an α energy of 3.5 MeV with either deuterium or tritium is with deuterium at an energy of 2.109 MeV. A series of resonant reactions can thus only be obtained by seeding the fuel with appropriate reactants. The only useful resonances of α particles below 3.5 MeV with light elements are the α-^{6}Li and α-^{7}Li resonances. The properties of these reactions are listed by Cecil et al.[4,5]

Now we calculate the total yield of resonant reactions for ICF targets. Let us assume a Breit–Wigner cross section [Eq. (7)] and neglect the nonresonant contribution to the total cross section. If we further assume that the stopping power changes little over the width of the resonance, it can be replaced by its value at the resonance energy E_R. For a narrow resonance ($\Gamma \ll E_R$), the de Broglie wavelength is also replaced by λ_R, its value at the resonance energy. Under these assumptions, the yield integrated over the total resonance is given by

$$Y = N_p \frac{N_A}{A_t} \frac{1}{|dE/d(\rho x)|_{E_R}} 2\pi^2 \lambda_R^2 \omega\gamma$$

$$= N_p \frac{N_A}{A_t} \frac{1}{|dE/d(\rho x)|_{E_R}} \frac{\Gamma}{2} \pi\sigma_R, \qquad (20)$$

where N_p is the total number of projectiles (in this case the number of α particles slowed down to the resonance energy), $\sigma_R \equiv \sigma(E_R)$ and the resonance strength $\omega\gamma$ is defined as

$$\omega\gamma = \frac{2J+1}{(2J_1+1)(2J_2+1)} \frac{\Gamma_{12}\Gamma_{34}}{\Gamma}. \qquad (21)$$

For mixed fuel, Eq. (20) changes in the same way as Eq. (11) does.

In Table I, the yield per α particle slowed down to the resonance energies for two fuel mixtures is given: 49% deuterium, 49% tritium, 1% ^{6}Li, 1% ^{7}Li and 40% deuterium, 40% tritium, 10% ^{6}Li, 10% ^{7}Li (these percentages refer to number densities). The stopping power makes the yield temperature and slightly density dependent. The calculation has been performed for temperatures of 1 and 5 keV and a density of 21 g/cm^3. Reducing the density by a factor of 10 increases the stopping power only by about 40% at 1 keV and about 20% at 5 keV. The stopping power decreases by about a factor of 5 when going from 1 to 5 keV. These dependencies are quite insensitive to the lithium contents. When going from 1% to 10% lithium, the γ-ray yield increases only by about a factor of 6 (not a factor of 10) because the same mass density was assumed in both calculations. For a 10% lithium contents, the γ-ray yield is of the order of 10^{-11}–10^{-9} per α particle.

The number of α particles at a certain reaction energy is determined from the detected γ-ray intensity, the resonance parameters and the stopping power. Since this last one is strongly temperature dependent, a good knowledge of the temperature is required. However, a qualitative picture of the α slowing can be obtained without good knowledge of the temperature because the relative variation of the stopping power with α energy is not strongly temperature dependent.

V. EXPERIMENTAL ASPECTS

A. Some detector aspects

γ rays from magnetically confined fusion plasmas have been detected with standard scintillation detectors.[4,7–10,15] The detection of γ rays from ICF targets demands a different concept because all γ rays are emitted in a very short

TABLE I. γ-ray yields of resonant α-capture reactions in deuterium-tritium ICF targets seeded with 1% and 10% ^{6}Li and ^{7}Li, for temperatures of 1 and 5 keV and a density of 21 g/cm^3. The yield is relative to the number of α particles slowed to the resonance energy E_R.

Reaction	E_R^a (MeV)	E_γ^b (MeV)	Y_γ/Y_α (10^{-12}) 1% ^{6}Li & ^{7}Li 1 keV	5 keV	10% ^{6}Li & ^{7}Li 1 keV	5 keV
α-D	2.109	2.186	15.3	80.7	9.33	48.9
α-^{6}Li	0.500(25)	4.056	11.3	60.2	84.9	446
	1.085	5.110	5.84	33.7	43.9	251
		4.392	2.77	16.0	20.8	119
		3.370	0.495	2.86	3.72	21.3
	1.175	5.164	1.61	9.49	12.1	69.1
		4.446	8.05	47.5	60.5	346
		3.010	23.2	137	174	995
		1.577	2.77	16.4	20.8	119
	2.435	5.920	7.48	36.5	56.3	273
		5.201	1.57	7.69	11.9	57.5
	2.605	6.025	12.7	59.6	96.0	446
α-^{7}Li	0.401(3)	8.920	2.63	13.2	19.6	96.5
		4.475	0.125	0.626	0.934	4.59
	0.814(2)	4.740	34.1	195	255	1450
		2.442	3.16	18.1	23.6	134
	0.953(2)	9.274	28.6	165	214	1220
		4.830	118	683	885	5070
		2.532	18.8	108	140	802

^{a}α energy in the laboratory system.
^{b}Center-of-mass γ-ray energy.

time (<1 ns). Also, since all γ rays travel at the same speed, time-of-flight techniques, commonly used for neutron energy measurements, are impossible. The measurement of a γ-ray spectrum therefore requires a detector that can detect a large number of individual γ rays at the same time. Several such detector concepts have been thought of and are briefly outlined in the following.

The most "classic" is a large detector array, such that each detector sees at most one γ ray. This type of neutron detection array using liquid scintillator is in use at Nova.[16,17] For γ rays, the scintillator would have to be NaI (best energy resolution), BaF$_2$ (fastest), or BGO (highest efficiency). More complex systems are thinkable, e.g., a BGO "core" to enhance the primary interaction of high-energy γ rays, surrounded by NaI to detect the secondary radiation, thus improving the overall energy resolution. Adding BaF$_2$ can provide a fast timing signal. Since the size of such an array has to increase with γ-ray energy, construction related limits will impose an upper limit on the detectable γ-ray energy.

Another detection scheme uses the fact that there is a one-to-one relationship between the energy and angle of a Compton scattered electron and the primary γ-ray energy. In this scheme, collimated γ rays impinge on a foil, thus creating Compton electrons in all directions. Using a conical slit, one selects the electrons scattered at just one angle. A CCD can record the position of these electrons after their trajectory has been bent by an electric or magnetic field. From this position distribution, the electron energy spectrum can be calculated and, using the known scatter-

ing angle, the γ-ray energy spectrum can be constructed. A good energy resolution requires a thin scattering foil and a narrow angle selection, resulting in a very small detection efficiency. For an electron energy resolution of 20 and 400 keV (at several MeV electron energy), the intrinsic efficiency is estimated to be only 6×10^{-6}, respectively 1.2×10^{-4}. This number does not include the solid angle covered by the scattering foil, which has to be very small as well.

A detailed picture of the γ-ray spectrum from ICF targets might be obtained from a heavy liquid bubble chamber. γ-ray energies are deduced from the path of the secondary electrons and positrons in the magnetic field. Holographic photography provides a large depth of field, has an excellent spatial resolution (8 μm measured,[18] 1.5 μm predicted,[19] in the plane perpendicular to the laser beam), and subsequently allows a large track density (estimated 50 000 tracks in a 25 cm diameter by 15 cm deep volume[19]) and a good γ-ray energy resolution. Therefore, this approach is very promising because a large number of γ rays can be detected individually in a small volume and with a good efficiency and energy resolution. A small heavy liquid bubble chamber is presently being built at Lawrence Livermore National Laboratory.

B. Neutron and γ-ray background

Since there are at least 10^7 times as many primary DT neutrons as there are α+T capture γ rays (see Fig. 3), it seems quite impossible to prevent any γ-ray detector from

being "flooded" by these neutrons. This suggests that in any case, γ-ray data will have to be obtained before the neutrons arrive at the detector.

From the maximum $\alpha + T$ γ-ray yield (about 10^{-7} per primary neutron) and the $D + T \rightarrow \gamma + {}^5He$ to $D + T \rightarrow n + \alpha$ branching ratio (5.5×10^{-5}) (Ref. 20) we deduce that the primary γ rays are at least 500 times more intense than the α-capture γ rays. Another source of contamination are neutron induced γ rays. For an $n + D \rightarrow \gamma + T$ cross section of 8 μb (at 14 MeV neutron energy),[21] the intensity ratio of these secondary γ rays to the primary neutrons is equal to $1.0 \times 10^{-9} \rho R$, with ρR expressed in mg/cm^2. The $n + T \rightarrow \gamma + {}^4H$ intensity is at least three times lower.[22] Because the 14 MeV neutron-induced breakup of D and T has a high cross section and creates high-energy protons (up to 12 MeV),[23] the $p + D \rightarrow \gamma + {}^3He$ tertiary reaction gives a non-negligible tertiary γ-ray intensity of $3 \times 10^{-9} \rho R$ (relative to the primary neutron yield). The $p + T \rightarrow \gamma + {}^4He$ yield is 300 times lower. The neutron induced γ-ray intensity from a plastic and/or glass target shell and any radiation connected to the $D + D$ fusion reaction products are negligible. The linear increase with ρR of the above given yields of secondary and tertiary reactions is only valid for small enough ρR (analogous to Fig. 3). The conclusion of all this is that a detector must mainly be shielded from or be able to discriminate primary γ rays. Although it can be an issue, we do not consider here neutron-induced γ rays from material in the vicinity of the target, since this cannot be treated in a general way. Collimation, however, will reduce this background.

VI. CONCLUSION

Two γ-ray diagnostics of the α slowing in ICF targets have been investigated. One is based on the $\alpha + T$ γ rays, the other uses a series of resonant α-capture reactions. Some experimental aspects and possible detection schemes were discussed. The calculated necessary yields are above those produced in present day targets. However, yields at a next generation ICF facility will allow γ-ray diagnostics, provided appropriate detectors are developed.

[1] D. E. Post, D. R. Mikkelsen, R. A. Hulse, L. D. Stewart, and J. C. Weisheit, J. Fusion Energy **1**, 129 (1981).

[2] Larry R. Grisham, Douglass E. Post, and David R. Mikkelsen, Nucl. Technol./Fusion **3**, 121 (1983).

[3] D. R. Slaughter, Rev. Sci. Instrum. **56**, 1100 (1985).

[4] F. E. Cecil, S. S. Medley, E. B. Nieschmidt, and S. J. Zweben, Rev. Sci. Instrum. **57**, 1777 (1986).

[5] F. E. Cecil, S. J. Zweben, and S. S. Medley, Nucl. Instrum. Method. Phys. Res. A **245**, 547 (1986).

[6] Vasilij G. Kiptilyj, Fusion Technol. **18**, 583 (1990).

[7] David E. Newman and F. E. Cecil, Nucl. Instrum. Method Phys. Res. **227**, 339 (1984).

[8] G. Sadler, O. N. Jarvis, P. van Belle, N. Hawkes, and B. Syme, Proceedings of the 14th European Conferences on Controlled Fusion and Plasma Heating, Madrid, Spain, June 22–26, 1987, Europhysics Conference Abstracts, Vol. III, p. 1232.

[9] F. E. Cecil and S. S. Medley, Nucl. Instrum. Method Phys. Res. A **271**, 628 (1988).

[10] Guy J. Sadler, Sean W. Conroy, Owen N. Jarvis, Pieter van Belle, J. Martin Adams, and Malcolm A. Hone, Fusion Technol. **18**, 556 (1990).

[11] Claus E. Rolfs and William S. Rodney, *Couldrons in the Cosmos* (The University of Chicago, Chicago, 1988).

[12] G. M. Griffiths, R. A. Morrow, P. J. Riley, and J. B. Warren, Can. J. Phys. **39**, 1397 (1961).

[13] M. D. Cable and S. P. Hatchett, J. Appl. Phys. **62**, 2233 (1987).

[14] D. V. Sivukhin, *Review of Plasma Physics* (Consultants Bureau, New York, 1966), Vol. 4, p. 93.

[15] K. W. Wenzel, R. D. Petrasso, D. H. Lo, C. K. Li, J. W. Coleman, J. R. Lierzer, E. Hsieh, and T. Bernat, Rev. Sci. Instrum. **63**, 4840 (1992).

[16] M. B. Nelson and M. D. Cable, Rev. Sci. Instrum. **63**, 4874 (1992).

[17] Michael D. Cable, S. P. Hatchett, and M. B. Nelson, Rev. Sci. Instrum. **63**, 4823 (1992).

[18] M. Dykes, P. Lecoq, D. Güsewell, A. Hervé, H. Wenninger, H. Royer, B. Hahn, E. Hugentobler, E. Ramseyer, and M. Boratav, Nucl. Instrum. Methods **179**, 487 (1981).

[19] Frederick R. Eisler, Nucl. Instrum. Methods **163**, 105 (1979).

[20] F. E. Cecil and F. J. Wilkinson, III, Phys. Rev. Lett. **53**, 767 (1984); F. E. Cecil, D. M. Cole, F. J. Wilkinson, III, and S. S. Medley, Nucl. Instrum. Method Phys. Res. B **10/11**, 411 (1985); G. L. Morgan, P. W. Lisowski, S. A. Wender, Ronald E. Brown, Nelson Jarmie, J. F. Wilkerson, and D. M. Drake, Phys. Rev. C **33**, 1224 (1986).

[21] G. Mitev, P. Colby, N. R. Roberson, H. R. Weller, and D. R. Tilley, Phys. Rev. C **34**, 389 (1986).

[22] S. Fiarman and W. E. Meyerhof, Nucl. Phys. A **206**, 1 (1973).

[23] G. Pauletta and F. D. Brooks, Nucl. Phys. A **255**, 267 (1975); E. Fuschini, C. Maroni, A. Uguzzoni, E. Verondini, and A. Vitale, Il. Nuovo Cimento B **48**, 1750 (1967).